doi:10.6041/j.issn.1000-1298.2016.11.025

Design and Performance Analysis of Soil Moisture Sensor Based on Capacitance Technology

Gao Zhitao[1,2] Liu Weiping[1,2] Zhao Yandong[1,2]

(1. *School of Technology*, *Beijing Forestry University*, *Beijing* 100083, *China*
2. *Beijing Laboratory of Urban and Rural Ecological Environment*, *Beijing Forestry University*, *Beijing* 100083, *China*)

Abstract: A kind of non-contact sensor based on capacitance method was designed. With the aid of the network vector analyzer, the probe of the sensor was measured in the organic solution with different dielectric constants, and the capacitance variation range of the ring probe of the sensor was determined as 7.08 ~ 22.75 pF. This paper formed 11 high-frequency ceramic capacitors with different capacitances respectively connected with 102 nH winding inductor in parallel into resonance circuit. Using the circuit to carry out experiment, the decision coefficient of test results and simulation results all reached 0.98. The measurement accuracy of the detection circuit met the sensor design requirements. Clay loam in Beijing area was chosen as experimental sample. The output of sensor detection unit and the corresponding measured values were carried out the polynomial fitting and linear fitting with a coefficient of determination of 0.995 9. The static and dynamic performance of the system can meet the soil moisture detection requirements. The effect of temperature on the output of the sensor was analyzed. The output of the sensor was fit with the temperature, and the coefficient was 0.987 9. The energy index K_a was further proposed. By the experiment, the influence ranges of longitudinal and transverse were identified as 10 cm and 5 cm. Finally, the comparison experiments showed that the proposed non-contact type moisture sensor was similar to that of the foreign products. It met the requirements of non-contact measurement of soil, at the same time, it had high cost-performance and laid the localization foundation for the similar products.

Key words: soil moisture sensor; capacitance method; non-contact; performance analysis

0 Introduction

The soil moisture content is the important factors that affect plant growth[1]. Commonly used soil moisture content detection methods are drying method, resistance method, tension meter method, neutron method and dielectric method, etc. Because of the rapid response, high safety and reliable performance of dielectric method, it has been widely used in agricultural research[2-8].

The sensor in use of dielectric method to measure the soil moisture content could be divided into contact measurement sensor and non-contact measurement sensor. Contact sensors in needle probe structure, generally should be buried in layers accordance with the depth of monitoring set. More typical sensors are ML3 ThetaProbe sensor of Delta-t in British, ECH2O series sensor of DECAGON in America, TRIME-HD2 TDR sensor of IMKO in Germany and the DB-Ⅲ soil moisture content sensor based on SWR principle that was independently researched and developed in Beijing Forestry University in domestic. A non-contact sensor uses a ring probe structure, which works in the pre-buried PVC pipe[9-10], such as soil moisture expansion line system of EnviroSCAN and soil moisture profile instrument of Diviner2000 of Sentek company. Compared with the contact measurement sensor, there are many advantages in convenient installation, no-damaged to the soil structure and easy replacement when non-contact measurement sensor is used[11-16]. However, it is difficult to analyze because of detection area around the non-contact sensor probe is more complex, therefore, the difficulty of product design is increasing. Although the performance of such products

Received date: 2016-04-20 Accepted date: 2016-05-09
Supported by National Science Foundation of China (Gront No. 31371537), Beijing Municipal Science and Technology Project (Z116100000916012) and Special Found for Beijing Common Construction Project
Corresponding author: Zhao Yandong, Professor, E-mail: yandongzh@bjfu.edu.cn. Tel: +86-010-62336956.

abroad has been recognized, but it is difficult to be widely used because of the high price, so it is very important to design non-contact sensor with high performance and low price with for promoting the application of sensors.

Base on above consideration, was a non-contact soil moisture sensor used the dielectric theory of capacitance method was designed according to the theory of parallel resonance.

1 Principle and structure of moisture sensor

1.1 Measurement theory

Using the capacitance method to measure the soil moisture content actually reflected the change of capacitance of ring probe in soil.

Detection principle and working environment is shown in Fig. 1.

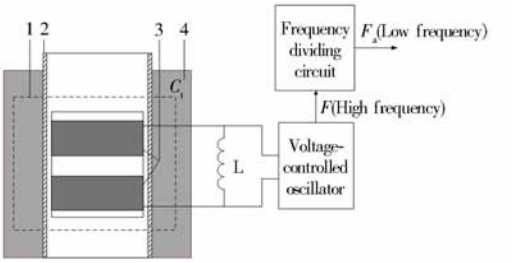

Fig. 1 Test environment and principle of soil moisture sensor

1. Probe 2. PVC pipe 3. Electrode receiving port of copper 4. Test soil

According to the parallel resonance theory[17-20]

$$f = \frac{1}{2\pi\sqrt{LC_t}} \tag{1}$$

where f is resonance frequency; L is parallel resonant inductance; C_t is induction capacitance of ring probe.

To characterize the change of capacitance of the ring probe, the change of parallel resonant frequency detection is needed. The capacitance of the non-contact sensor is related to filled media, as

$$C_t = g\varepsilon_r\varepsilon_0 \tag{2}$$

where g is constants related to shape size; ε_r is dielectric constant of medium filled around ring probe; ε_0 is dielectric constant in vacuum.

Soil is a kind of porous media, and its relative dielectric constant as in complex domain could be calculated

$$\varepsilon_r = \varepsilon' - \mathrm{j}\varepsilon'' \tag{3}$$

where ε' is the real part of the dielectric constant which represents energy storage; ε'' is the imaginary part of the dielectric constant which refers to the loss of total energy storage.

The imaginary part of the dielectric constant is mainly composed of dielectric relaxation loss coefficient of ε_d'' and ionic conductivity of σ, namely

$$\varepsilon'' = \varepsilon_d'' + \frac{\sigma}{2\pi f\varepsilon_0} \tag{4}$$

$$\varepsilon_r = \varepsilon' - \mathrm{j}\left(\varepsilon_d'' + \frac{\sigma}{2\pi f\varepsilon_0}\right) \tag{5}$$

On both sides of Eq. (5) multiplied by $g\varepsilon_0$, the following information were obtained

$$C_t = C^* - \mathrm{j}\left(\frac{g\sigma}{\omega} + g\varepsilon_d''\varepsilon_0\right) \tag{6}$$

$$\mathrm{j}\omega C_t = \mathrm{j}\omega C^* + (g\sigma + g\omega\varepsilon_d''\varepsilon_0) \tag{7}$$

$$G = g\sigma + g\omega\varepsilon_d''\varepsilon_0 \tag{8}$$

$$\mathrm{j}\omega C_t = \mathrm{j}\omega C^* + G \tag{9}$$

where C^* is the real part of capacitance of the ring probe; G is dielectric loss the ring probe.

The conclusion was arrived in the light of Eq. (8), which revealed the dielectric loss was mainly affected by conductivity and polarization of soil. According to previous research, the influence of the dielectric loss ε on the change of impedance of the probe could be neglected during the analysis when the conductivity of the soil leaching solution was very low. Since the conductivity of the leaching solution of the test soil was lower than 0.20 mS/cm, the dielectric loss ε is neglected.

Taking the impact of stray capacitance and PVC pipe on the circuit in measurement process into account, the parameters C_P and C_S are added in the circuit. The resonant circuit model of the moisture sensor is shown in Fig. 2.

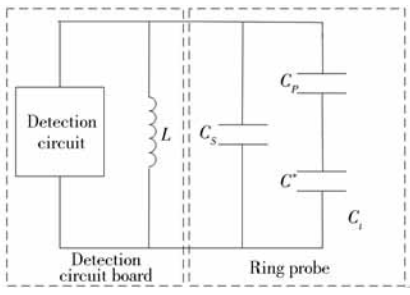

Fig. 2 Equivalent circuit for capacitance probe sensor

The capacitive reactance C_t of the sensor ring probe in Fig. 2 can be expressed as

$$C_t = C_S + \frac{C_P C}{C_P + C} \tag{10}$$

where C_S is stray capacitance of the sensor ring probe; C_P is capacitance of PVC pipe.

Further concluded

$$f_o = \frac{1}{2\pi \sqrt{L\left(C_S + \frac{C_P C}{C_P + C}\right)}} \tag{11}$$

where f_0 is output frequency of the sensor.

The parallel resonant inductance and the induction capacitance of the PVC pipe are fixed during the measurement, which could be seen from Eq. (11). So the change of output frequency is mainly affected by the induction capacitance C^* of soil.

1.2 Hardware circuit structure

The non-contact soil moisture sensor designed consists of two parts: sensor probe and detection circuit. The sensor probe is cylindrical, the outside of which embedded with two brass ring electrode, and the two electrodes, the diameter and height of which are 25mm , were separated by 15mm. The detection circuit board and the brass electrode are fixed to the inside of the probe through the metal wire connected. This non-contact sensor in the PVC pipe which preliminarily buried in soil needs to be equipped with a dedicated collection device to work[22]. The system, which mainly consisted of the resonant unit made of voltage-controlled oscillator, shaping circuit unit, frequency division unit, STM8 microcontroller unit, the temperature detection unit and D/A conversion unit, is shown in Fig. 3.

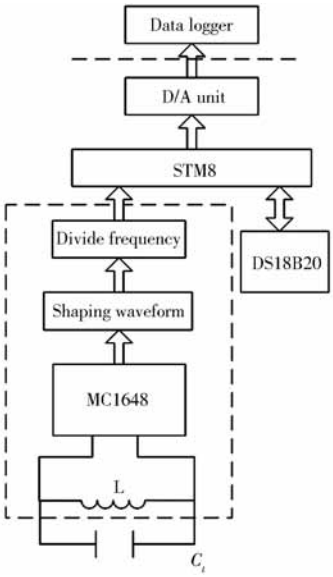

Fig. 3 Principle diagram of test panel system

The ring probe, as a parallel resonant circuit capacitor, generated high-frequency signal under the action of voltage-controlled oscillator, the high-frequency signal was turned into low-frequency signal of 2 ~ 4 kHz and sent to the microcontroller by means of the shaping and frequency dividing. According to the normalized fitting model of the output frequency and the volume moisture content and with the compensation of temperature obtained by the temperature detection unit, the microcontroller commanded D/A module (DAC7571) to convert frequency output of the moisture detection circuit into a voltage output of 0 ~ 2 500 mV.

2 Characteristics analysis for capacitive reactance of soil moisture sensor

In the design of soil moisture based on the capacitance method, it is of great importance to run the characteristics analysis for capacitive reactance of the ring probe. In this paper, with the help of a high-frequency vector network analyzer (NA7300 type, 50 Ω, Tianjin Deli Electronic Instrument Company, the scanning frequency was 0.3 ~ 3 000 MHz and the frequency resolution was 10 Hz), the capacitance characteristic of ring probe in 9 media were analyzed. In the test, frequency was 100 MHz and the reflection method was applied and the temperature was 20℃. Totaly 9 kinds of media and its corresponding dielectric constant were shown in Tab. 1.

Tab. 1 Dielectric constant of organic solution (20℃)

Medium	Dielectric constant
Air	1.0
Ethylacetate	6.02
Isoamylol	15.19
N-butyl alcohol	17.51
Isopropyl alcohol	19.92
Alcohol	24.55
Alcohol:water(2:1)	43.6
Alcohol:water(1:1)	53.3
Distilled water	81.00

Firstly, the reagent were put into a PVC testing tube, which height and diameter were 20 cm, in which a PVC pipe with height of 20 cm and diameter of 5.6 cm was fixed at the center. Then, the test cable of the vector network analyzer and the ring probe were connected using the connector. The vector network analyzer was calibrated with a load of 50 Ω in open and

short circuit after powered up for 1 h. Finally, the ring probe was put into the PVC pipe to measure the capacitance. In the experiment, the test result was average of 5 times, thus reducing the operation error. The test results were shown in Fig. 4.

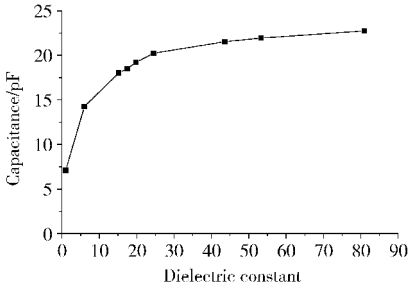

Fig. 4 Effect of dielectric constant on capacitance characteristics of ring probe

As can be seen from Fig. 4, capacitance of the ring probe and the dielectric constant of the surrounding filled showed a monotonic non-linear relationship. When the range of the dielectric constant was 0 ~ 15, the curve was sharply rose and the corresponding range of capacitance of sensor was 7.08 ~ 16.5 pF, and then curve change was significantly slowed. When the range of the dielectric constant was 1 ~ 81, the changing range of capacitance was 7.08 ~ 22.75 pF.

3 Measurement accuracy test of detection circuit

The sensor used the principle of parallel resonance to detect the soil moisture content. The ring probe of sensor was equivalent to a capacitor and resonant inductance determined the test frequency. Taking into account the probe capacitance and the test frequency would be affected by the conductivity and other factors, finally, the 102 nH high-frequency winding inductance was selected as the resonant inductor. During the test, 11 kinds of high-frequency ceramic capacitors simulated the sensor probe and placed in detection circuit. The output frequency and capacitance were shown in Tab. 2 and Fig. 5.

Tab. 2 Capacitance and resonance frequency

Capacitance/pF	5	10	12	15	18	20	22	30	33	39	47	56
Resonance frequency/MHz	220.750	150.546	138.336	128.042	113.250	110.920	110.161	90.682	85.588	79.384	73.701	67.464

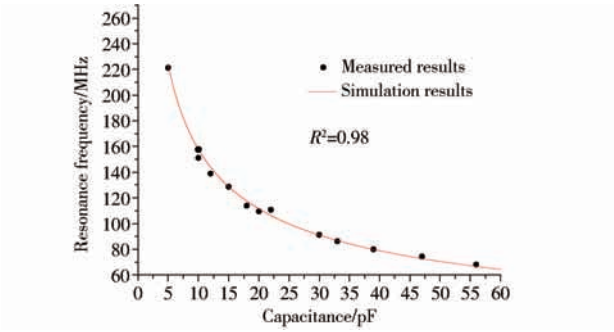

Fig. 5 Test and operation results of resonance frequency in different capacitances

It can be seen from Fig. 5, the determination coefficient of the results was measured by detection circuit and the simulation results of Eq. 1 was 0.98, that indicated the detection circuit could accurately measure the induction capacitance. The resonant frequency decreased monotonically as the capacitance increased. When the range of capacitance of sensor probe was 7.07 ~ 22.75 pF (the maximum variation in soil), the range of resonant frequency was 188 ~ 104 MHz. According to previous research, when frequency was 188 ~ 104 MHz, the effect of soil salinity on the measurement results could be effectively reduced[24].

4 Performance analysis of sensor

4.1 Test of dynamic response performance

The dynamic response performance is an important index of sensor in the application. It is the time that the sensor output from changing to stable when the soil moisture content changed around the detection area. The test equipment was a PVC testing tube with a PVC pipe fixed in the center. Firstly, place the sensor in the PVC pipe and fill the PVC testing tube with water, the time of the sensor output from the powered to the stability was 50 ms, which was obtained by the rising edge capture function of the oscilloscope single trigger. Then, the sensor was quickly pulled out from the PVC pipe, the time of the sensor output from changing to stability was 150 ms.

4.2 Calibration of sensor

In the sensor design, the calibration is a very important part. The frequency signal of output from the moisture detection circuit needs to be normalized before the sensor was calibrated. The normalization method is as follows

$$V_O = V_C \frac{f_A - f_M}{f_A - f_W} \tag{12}$$

where f_A is the frequency of outputs of the moisture detection circuit when the sensor was respectively placed in air; f_W is the frequency of outputs of the moisture detection circuit when the sensor was respectively placed in water; f_M is the frequency of outputs of the moisture detection circuit when the sensor was respectively placed in measured soil; V_C is reference voltage of 2 500 mV.

The frequency signal of sensor output turned into voltage signal of 0 ~ 2 500 mV after the normalization.

The soil sample was a typical clay loam from the nursery of Beijing Forestry University (116°21′14″E, 40°0′54″N) and conductivity of leaching solution was 0.20 mS/cm. The compositions of the sample were 11% of sand, 71% of powder and 18% of clay (they were mass fraction). The samples were firstly air-dried and screened (screen's pore radius was 0.4 mm). And then it was dried in a drying oven (105℃, 24 h). Tatolly 9 kinds of the soil testing samples with different volumetric moisture contents were prepared. The samples, in density of 1.6 g/cm^3, were uniformly filled in 9 PVC test tube that height was 20 cm and diameter was 30 cm. Each tube was placed with a PVC pipe with height of 40 cm and diameter of 5.6 cm. After standing for 48 h, to take off the soil samples, the soil volumetric moisture contents of the 9 test tubes were determined by the drying method, and the test results respectively were 1.5%, 8.05%, 11.08%, 18.02%, 23.56%, 28.77%, 33.58%, 36.75% and 40.01%. The test ambient temperature was 10℃. The calibration environment was shown in Fig. 6. The sensor output voltage was run polynomial fitting that collected by a dedicated acquisition device. The results were shown in Fig. 7.

Fig. 7 revealed that the correlation between output of the sensor and the soil moisture content was very tight,

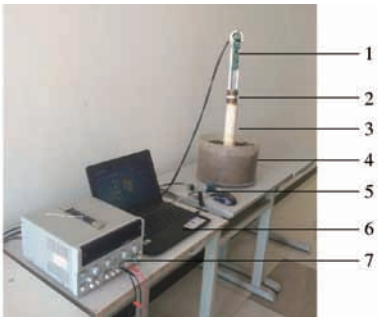

Fig. 6 Sensor calibration environment

1. Data logger 2. Ring sensor 3. PVC pipe 4. PVC tube 5. RS485-RS232 6. Computer 7. Power

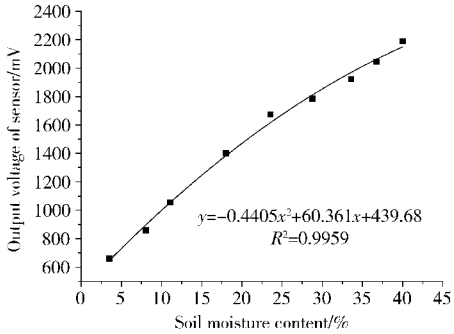

Fig. 7 Calibration results of moisture sensor

and the determination coefficient R^2 reached 0.995 9. At the same time, it obviously can be seen sensitivity of the sensor was very high, that was, the soil volumetric moisture content changed each of 10% there was more than 600 mV voltage outputted.

4.3 Effect of temperature on sensor output

Taking into account of the sensor in using, the output voltage might be affected by the environment temperature, in this paper, the sensor temperature calibration was designed.

Firstly, the distilled water were put into the PVC testing tube, of which height and diameter were 20 cm, in which a PVC pipe with height of 20 cm and diameter of 5.6 cm was fixed at the center. The soil moisture sensor was placed in PVC pipe and insulation cotton was used at upper and lower ends of the PVC pipe to prevent the heat from flowing.

Next, the PVC test tube was sealed with a plastic film, and a mercury thermometer was inserted into the water. And then the PVC test tube was placed into an oven.

Finally, the oven's temperature was adjusted to a gradient of 10 ~ 50℃ at mterral of 5℃. When the temperature of the mercury thermometer was consistent with setting temperature of the oven, the voltage of the sensor was recorded. The test results were shown in Fig. 8.

As shown in Fig. 8, the output of the sensor and the soil moisture content had good correlation and the determination coefficient R^2 reached 0.987 9. The output of the sensor increases by about 2.903 3 mV for every 1℃ rising. The main reason for the voltage rise was that the dielectric constant of the filled media around the probe was affected by the temperature and the change of electrical characteristics of the electronic components in the circuit was caused by the change of temperature. Considering the sensor output was

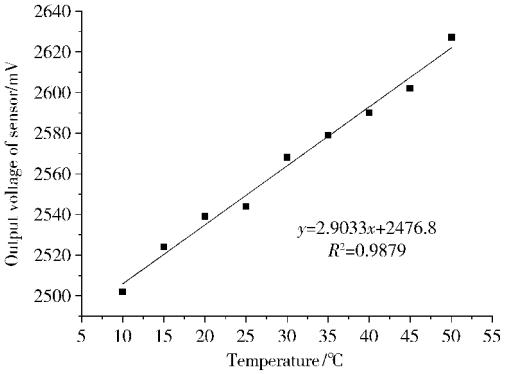

Fig. 8 Changes of sensor output with temperature

affected by temperature changes, the temperature detection function was configured in the soil moisture sensor. So that sensor output was corrected according to the real-time temperature. In order to improve the versatility of the sensor, because of the output interface of moisture sensor didn't provide the temperature output function, this design only for a single moisture sensor compensated on the temperature. This solution could only reduce the effect of temperature on sensor output in a certain extent, in order to obtain more accurate measurements, the user should establish a mathematical model of different gradient of soil based on the type of soil for analysis[22].

4.4 Test for sensitivity of sensor

4.4.1 Longitudinal effect area of sensor

The measurement sensitive area of sensor represented measurement range, was an important indicator of sensor performance. The test soils, with volumetric moisture content of 16%, 20% and 25%, were prepared according to the method shown in Seition 4.2. The soil samples were sequentially loaded into 3 PVC test tube with height of 20 cm and diameter of 30 cm in which a PVC pipe with height of 20 cm and diameter of 5.6 cm was fixed at the center. Using plastic wrap sealed the PVC test tube to standing 64 h.

The soil moisture sensor was placed in the PVC pipe which was fixed in the center of PVC test tube in that configured with the soil samples. The center of the sensor was 10cm away from the upper surface of the soil. The sensor was moved upwards at 1 cm gradient, and the voltage of sensor at each gradient was recorded. The test results of 3 soils with different moisture contents were shown in Fig. 9.

Fig. 9 showed that in the process of the sensor in the PVC pipe moving up, the output voltage of the sensor monotonically reduced with the increase of moving

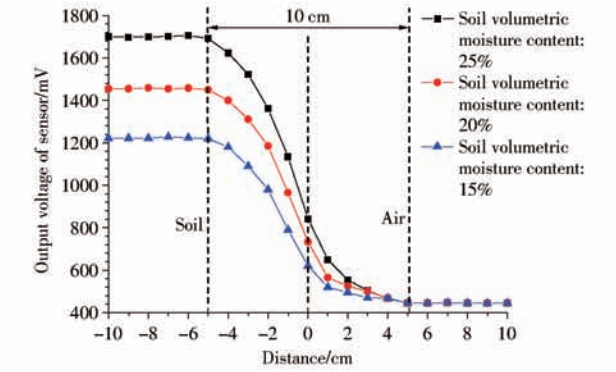

Fig. 9 Experimental results of axial sensitivity for sensors

distance. The soil volumetric moisture content didn't had much impact of the sensor's longitudinal effect area. The longitudinal effect area of the sensor was 10cm. In order to ensure the accuracy of the measurement data, the sensor designed should be placed at a distance of 5cm below the soil surface.

4.4.2 Lateral effect area of sensor

The soil moisture sensor was placed in PVC pipe to measure the moisture content of the soil in the test tube that using a knife to change thickness (the distance from the wall of the PVC testing tube to the soil edge) at gradient of 1 cm and the voltage of the sensor output was recorded. The test process was shown in Fig. 10.

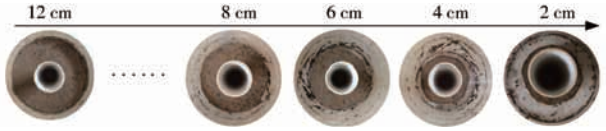

Fig. 10 Experiment of relative radial sensitivity measurement of sensors

In order to more intuitively realize the effect of soil thickness on the output voltage of the sensor, this paper presented an energy index K_a to characterize the energy distribution of the transverse radius of the sensor, as

$$K_a = \frac{V_C - V_{PVC}}{V_{soil} - V_{PVC}} \tag{13}$$

where V_{soil} is the voltage of the sensor in soil with a thickness of 12 cm, V_{PVC} is voltage of sensor in the PVC pipe (PVC pipe surrounded air), V_C is the real-time measured value of the sensor.

The test results of the sensor in 16%, 20% and 25% volumetric moisture content were shown in Fig. 11.

Fig. 11 showed the energy index reduced with the increase of thickness of the surrounding soil. The 99% of the energy was distributed within 5 cm of the outer wall of the PVC testing tube for all three gradient soils.

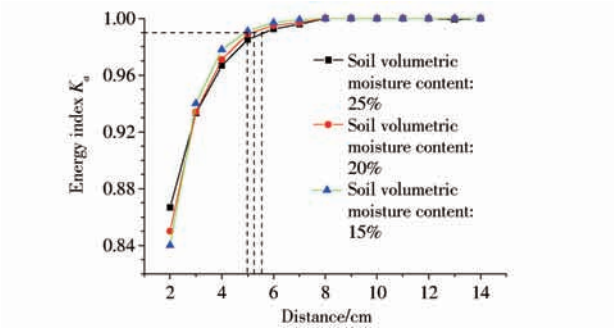

Fig. 11 Experimental results of relative radial sensitivity of sensors

Therefore, the lateral effect area of the non-contact soil moisture sensor designed in this paper was 5 cm.

5 Contrast test and result analysis

In order to analyze the performance gap between the soil non-contact sensor and such products abroad, the sensor contrast test was designed. The sensor was compared with soil moisture expansion line system of EnviroSCAN with a range of 0 ~ 100% and an accuracy of ±2%. Toully 7 soil samples with the soil volumetric moisture contents of 5.4%, 10.4%, 16.3%, 23.9%, 28.6%, 32.3%, and 36.5% were prepared according to the test process in Section 4.2, two sensors were used for the measurement. The results of soil non-contact sensor and EnviroSCAN were shown in Tab. 3.

Tab. 3 Comparative experiments with EnviroSCAN soil moisture systems %

No.	1	2	3	4	5	6	7
EnviroSCAN	5.32	10.61	17.11	24.51	27.65	33.56	36.22
Sensor	5.43	9.92	16.01	23.31	28.62	32.28	35.57
Absolute error	−0.11	0.69	1.10	1.20	−0.63	1.28	0.65
Relative error	−2.1	6.5	6.4	4.9	−2.3	3.8	1.8

As it can be seen from Tab. 3, the absolute error of the soil volumetric water content was −0.61% ~ 1.20% and the relative error was −2.3% ~6.5%. The absolute error between the two was less than 2%, indicating that the performance of the two sensors was equivalent.

6 Conclusion

(1) A non-contact soil moisture sensor was designed to monitor the soil moisture in real time.

(2) The capacitance characteristics of the ring probe and the performance of the detection circuit were studied. The capacitance of the ring probe was analyzed using the network vector analyzer in 9 kinds of organic solution, and it is determined that the dielectric constant from 1 to 81 of ring probe presented the range of capacitance was 7.08 ~ 22.75 pF. The experiment results showed that the accuracy of the sensor circuit was satisfied with the requirements of sensor through the paralleled with 11 kinds of capacitance of the high-frequency ceramic capacitor in parallel resonant experiments.

(3) From the calibration and correlation test results it could be seen, the sensor accuracy, sensitivity and dynamic response performance could meet the sensor design requirements.

(4) The energy index K_a was proposed. The measuring range of the sensor was obtained by test. The longitudinal range was 10 cm, and the lateral effect range was 5 cm.

(5) The comparison test showed that the detection precision of the designed soil non-contact moisture sensor was similar to that of the products at abroad. The absolute error of volumetric moisture content was −0.61% ~ 1.20%, and the relative error was −2.3% ~6.5%.

References

[1] LI Lianjun, SUN Yurui, LIN Jianhui. A wireless-sensor for soil water content powered by solar energy [J]. Journal of Jiangsu University: Natural Science Edition, 2009, 30(6): 541 −544. (in Chinese)

[2] KANG S, ZHANG J. Controlled alternate partial root-zone irrigation: Its physiological consequences and impact on water use efficiency [J]. Journal of Experimental Botany, 2004, 55(407): 2437 −2446.

[3] HUTTON R J, LOVEYS B R. A partial root zone drying irrigation strategy for citrus-effects on water useefficiency and fruit characteristics [J]. Agricultural Water Management, 2011, 98(10):1485 −1496.

[4] HEDLEY C B, YULE I J. A method for spatial prediction of daily soil water status for precise irrigation scheduling [J]. Agricultural Water Management, 2009, 96(12): 1737 −1745.

[5] THOMPSON R B, GALLARDE M, VALDEZ L C, et al. Using plant water status to define threshold values for irrigation management of vegetable crops using soil moisture sensors [J]. Agricultural Water Management, 2007, 88(1 −3):147 −158.

[6] GAO Xiaodong, WU Pute, ZHAO Xining, et al. Estimating the spatial means and variability of root-zone

soil moisture in gullies using measurements from nearby uplands[J]. Journal of Hydrology, 2013, 476(1): 28 - 41.

[7] ZHANG Xueli, HU Zhenqi, CHU Shili. Methods for measuring soil water content: a review[J]. Chinese Journal of Soil Science, 2005, 36(1): 118 - 121. (in Chinese)

[8] CAI Kun, YUE Xuejun, HONG Tiansheng, et al. Design of soil water content sensor based on phase-frequency characteristics of RC networks[J]. Transactions of the CSAE, 2013, 29(7): 36 - 43. (in Chinese)

[9] DEAN T J, BELL J P, BATY A J B. Soil moisture measurement byan improved capacitance technique: Part I. sensor design and performance[J]. Journal of Hydrology, 1987, 93(1 - 2): 67 - 78.

[10] PALTINEANU I C, STARR J L. Real-time soil water dynamics using multi sensor capacitance probes: Laboratory calibration[J]. Soil Science Society of America Journal, 1997, 61(6): 1576 - 1585.

[11] SHENG W, SUN Y, LAMMERS P S, et al. Observing soil water dynamics under two field conditions by a novel sensor system[J]. Journal of Hydrology, 2011, 409(1 - 2): 555 - 560.

[12] LI Xiaodong, WU Yongfeng, LI Guanglin, et al. Development of wireless soil moisture sensor based on solar energy[J]. Transactions of the CSAE, 2010, 26(11): 13 - 18. (in Chinese)

[13] ZHAO Yandong, MA Yangfei, WANG Yongzhi. Green land precision irrigation control system and analysis of optimal irrigation amount[J]. Translations of the Chinese Society for Agricultural Machinery, 2012, 43(3): 46 - 50. (in Chinese)

[14] STEVEN R, ROBERT C, JOAQUIN J, et al. Soil water sensing for water balance, ET and WUE[J]. Agricultural Water Management, 2012, 104(2): 1 - 9.

[15] ZHAO Yandong, WANG Yiming. Intelligent system of measuring the spatial distributions of Soil moisture[J]. Transactions of the Chinese Society for Agricultural Machinery, 2005, 36(2): 76 - 78. (in Chinese)

[16] PENG Zengyu, ZHAO Yandong. A monitoring system of real-time soil water content based onμC/OS - Ⅱ operating system[J]. Journal of Beijing Forestry University, 2010, 32(6): 114 - 119. (in Chinese)

[17] GASKIN G J, MILLER J D. Measurement of soil water content using a simplified impedance measuring technique[J]. Journal of Agricultural Engineering Research, 1996, 63(2): 153 - 159.

[18] VELAZQUEZ M B, GRACIA L C, PLAZA G P J. Determination of dielectric properties of agricultural soil[J]. Biosystems Engineering, 2005, 91(1): 119 - 125.

[19] KIZITI F, CAMPBELL C S, CAMPBELL G S, et al. Frequency, electrical conductivity and temperature analysis of a low-cost capacitance soil moisture sensor[J]. Journal of Hydrology, 2008, 352(3 - 4): 367 - 378.

[20] WOJCIECH S, ANDRZEJ W. A FDR sensor for measuring complex soil dielectric permittivity in the 10 ~ 500 MHz frequency range[J]. Sensors, 2010, 10(4): 3314 - 3329.

[21] MA Daokun, SUN Yurui, WANG Maohua, et al. Three-dimensional numerical modeling of a four-pin probe for soil water content[J]. Australian Journal of Soil Research, 2006, 44(2): 183 - 189.

[22] GAO Zhitao, LIU Weiping, ZHAO Yandong, et al. Design and performance analysis of a multilayer composite sensor for soil profile[J]. Transactions of the Chinese Society for Agricultural Machinery, 2016, 47(1): 108 - 117. (in Chinese)

[23] ZHAO Yandong, GAO Chao, ZHANG Xin, et al. Non-destructive measurement of plant stem water content based on standing wave ratio[J]. Transactions of the Chinese Society for Agricultural Machinery, 2016, 47(1): 310 - 316. (in Chinese)

[24] NADLER A, LAPID Y. An improved capacitance sensor for in situ monitoring of soil moisture[J]. Soil Research, 1996, 34(3): 361 - 368.

doi:10.6041/j.issn.1000-1298.2016.11.025

基于电容法的非接触式土壤水分传感器设计与性能分析

高志涛[1,2]　刘卫平[1,2]　赵燕东[1,2]

(1.北京林业大学工学院,北京 100083;2.北京林业大学城乡生态环境北京实验室,北京 100083)

摘要:针对接触式土壤水分传感器存在对土体破坏大及使用安装、更换困难等问题,设计了一种基于电容法的非接触式土壤水分传感器。借助网络矢量分析仪对传感器环形探头在不同介电常数的有机溶液中进行测量,确定了传感器环形探头电容变化范围为 7.08 ~ 22.75 pF。选取 11 种不同电容值高频瓷片分别与 102 nH 的绕线电感进行并联谐振试验,得到的测试结果与仿真结果的决定系数达到了 0.98,检测电路的测量精度能够满足传感器的设计要求。以北京地区粘壤土作为测试样本,对传感器输出与对应的测量值进行了多项式拟合,决定系数达到了 0.995 9,系统的稳态与动态性能均能满足土壤水分的检测要求。通过试验分析了温度对传感器输出的影响,将传感器输出结果与温度进行线性拟合,决定系数达到了 0.987 9。进一步提出了能量指数 K_a,通过试验的方式确定了传感器的纵向影响范围为 10 cm,横向影响范围为 5 cm。最后对比试验表明,所设计的土壤非接触式水分传感器与国外同类产品性能相当,能够满足土壤非接触式测量的要求,但具有更高的性价比,为同类产品的国产化奠定了基础。

关键词:土壤水分传感器;电容法;非接触式;性能分析

中图分类号:S237　　**文献标识码**:A　　**文章编号**:1000-1298(2016)11-0185-07

Design and Performance Analysis of Soil Moisture Sensor Based on Capacitance Technology

Gao Zhitao[1,2]　Liu Weiping[1,2]　Zhao Yandong[1,2]

(1. *School of Technology*, *Beijing Forestry University*, *Beijing* 100083, *China*

2. *Beijing Laboratory of Urban and Rural Ecological Environment*, *Beijing Forestry University*, *Beijing* 100083, *China*)

Abstract: A kind of non-contact sensor based on capacitance method was designed. With the aid of the network vector analyzer, the probe of the sensor was measured in the organic solution with different dielectric constants, and the capacitance variation range of the ring probe of the sensor was determined as 7.08 ~ 22.75 pF. This paper formed 11 high-frequency ceramic capacitors with different capacitances respectively connected with 102 nH winding inductor in parallel into resonance circuit. Using the circuit to carry out experiment, the decision coefficient of test results and simulation results all reached 0.98. The measurement accuracy of the detection circuit met the sensor design requirements. Clay loam in Beijing area was chosen as experimental sample. The output of sensor detection unit and the corresponding measured values were carried out the polynomial fitting and linear fitting with a coefficient of determination of 0.995 9. The static and dynamic performance of the system can meet the soil moisture detection requirements. The effect of temperature on the output of the sensor was analyzed. The output of the sensor was fit with the temperature, and the coefficient was 0.987 9. The energy index K_a was further proposed. By the experiment, the influence ranges of longitudinal and transverse were identified as 10 cm and 5 cm. Finally, the comparison experiments showed that the proposed non-contact type moisture sensor was similar to that of the foreign products. It met the requirements of non-contact measurement of

收稿日期:2016-04-20　修回日期:2016-05-09

基金项目:国家自然科学基金项目(31371537)、北京市科技计划项目(Z116100000916012)和北京市共建项目专项

作者简介:高志涛(1989—),男,博士生,主要从事生态信息智能检测与控制研究,E-mail:e228319@163.com

通信作者:赵燕东(1965—),女,教授,博士生导师,主要从事生态信息智能检测与控制研究,E-mail:yandongzh@bjfu.edu.cn

soil, at the same time, it had high cost-performance and laid the localization foundation for the similar products.

Key words: soil moisture sensor; capacitance method; non-contact; performance analysis

引言

土壤含水率是影响植物生长的重要因素[1]。常用的土壤含水率检测方法有烘干法、电阻法、张力计法、中子仪法和介电法等。介电法因其响应速度快、安全性高、性能可靠等优点已经被广泛应用于农业研究中[2-8]。

在利用介电法测量土壤含水率的传感器中,可以依据使用方法分为接触式测量传感器与非接触测量传感器。接触式传感器一般采用针式探头结构,使用时需要按照监测深度分层埋设。比较常见的典型传感器有英国 Delta-t 公司生产的 ML3 ThetaProbe 型传感器、美国 DECAGON 公司生产的 ECH2O 系列传感器、德国 IMKO 公司的 TRIME-HD2 TDR 型土壤水分传感器以及国内北京林业大学自主研发的基于 SWR 原理的 BD-III 型土壤水分传感器。非接触传感器一般采用环式探头结构,其工作于预先埋设的 PVC 管体中[9-10]。如 Sentek 公司的 EnviroSCAN 型土壤水分扩线系统与 Diviner2000 型土壤水分廓线仪。相比于接触式测量传感器,非接触式测量传感器具有施工方便、不破坏土壤结构、传感器损坏更换简单等优点[11-16]。但是由于非接触式传感器探头周围检测区域比较复杂,很难用现有的介电模型进行分析,因此增加了产品设计的难度。国外的此类产品虽然在性能方面得到了认可,但是因其价格高昂很难得到广泛应用,所以设计一款高性能与低价格的非接触传感器对传感器的大面积推广具有十分重要的意义。

基于以上考虑,本文利用介电理论中的电容法,依据并联谐振理论设计一种非接触式土壤水分传感器。

1 水分传感器的测量原理与结构

1.1 测量原理

利用电容法测量土壤含水率实际上反映的是土壤环境中环形探头容值的变化。检测原理与工作环境如图 1 所示。

根据并联谐振理论[17-20],有

$$f=\frac{1}{2\pi\sqrt{LC_t}} \tag{1}$$

式中 f——谐振频率 L——并联谐振电感

C_t——环形探头的感应电容

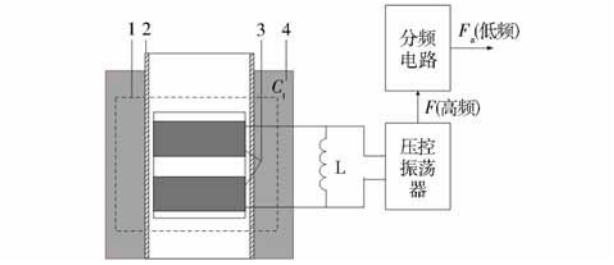

图 1 传感器测试环境与原理图

Fig. 1 Test environment and principle of soil moisture sensor

1. 探头测量区域 2. PVC 管 3. 黄铜电极 4. 测量土体

通过检测并联谐振频率 f 变化来表征传感器环形探头容值的变化。

非接触式传感器环形探头的电容与其内部的填充物质的介电常数有关,即

$$C_t=g\varepsilon_r\varepsilon_0 \tag{2}$$

式中 C_t——环形探头电容

g——与形状尺寸有关的常数

ε_r——探头周围填充介质的介电常数

ε_0——真空中的介电常数

土壤作为一种多孔介质,其相对介电常数 ε_r 在复数域内可表示为

$$\varepsilon_r=\varepsilon'-\mathrm{j}\varepsilon'' \tag{3}$$

式中 ε'——介电常数的实部

ε''——介电常数的虚部

介电常数的虚部 ε'' 主要由介电弛豫损耗系数 ε_d'' 与离子电导率 σ 两部分组成,即

$$\varepsilon''=\varepsilon_d''+\frac{\sigma}{2\pi f\varepsilon_0} \tag{4}$$

则

$$\varepsilon_r=\varepsilon'-\mathrm{j}\left(\varepsilon_d''+\frac{\sigma}{2\pi f\varepsilon_0}\right) \tag{5}$$

对式(5)两边同时乘以 $g\varepsilon_0$,进一步得出

$$C_t=C^*-\mathrm{j}\left(\frac{g\sigma}{\omega}+g\varepsilon_d''\varepsilon_0\right) \tag{6}$$

$$\mathrm{j}\omega C_t=\mathrm{j}\omega C^*+(g\sigma+g\omega\varepsilon_d''\varepsilon_0) \tag{7}$$

$$G=g\sigma+g\omega\varepsilon_d''\varepsilon_0 \tag{8}$$

$$\mathrm{j}\omega C_t=\mathrm{j}\omega C^*+G \tag{9}$$

式中 C^*——环形探头电容的实部

G——环形探头的介电损耗

由式(8)可知介电损耗 G 主要受土壤介质的电导率 σ 与土壤本身的极化作用两方面的影响。根据前人研究结果,在土壤浸出液电导率很低的时候,分析过程中可以忽略介电损耗 G 对探头整体阻抗变化的影响[21]。因本文涉及试验土壤的浸出液电

导率低于 0.20 ms/cm，所以忽略了介电损耗 G 对测量的影响。

考虑到在测量过程中 PVC 外管与电路杂散电容对电路的影响，在电路中增加了参数 C_P 与 C_S。本文研究的水分传感器的谐振电路模型如图 2 所示。

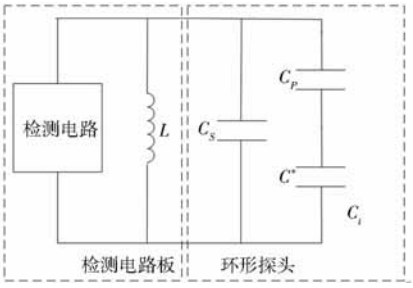

图 2　电容式传感器等效电路图

Fig. 2　Equivalent circuit for capacitance probe sensor

图 2 传感器环形探头的容抗 C_t 可表示为

$$C_t = C_S + \frac{C_P C}{C_P + C} \tag{10}$$

式中　C_S——环形探头所分布的杂散电容

C^*——测量土壤的表征电容

C_P——PVC 管所表征的电容

进一步得出

$$f_o = \frac{1}{2\pi\sqrt{L\left(C_S + \frac{C_P C}{C_P + C}\right)}} \tag{11}$$

其中　$\omega = 2\pi f$

式中　f_o——传感器的输出频率

通过式(11)可知，并联谐振电感 L 与 PVC 管感应电容 C_P 在测量过程中是固定不变的。所以输出频率 ω 的变化主要受土壤区域感应电容 C^* 的影响。

1.2　硬件电路结构

本文所设计的非接触式土壤水分传感器由传感器探头与检测电路两部分组成。传感器探头外形呈圆柱状，其外侧嵌有 2 个黄铜制成的圆环电极(直径 25 mm，高 25 mm)，2 个电极之间相距 15 mm。检测电路板与黄铜电极通过金属导线连接固定在探头内侧。此非接触式传感器工作于事先埋设的 PVC 管体中，需要与专用的采集设备配套使用[22]。其系统框图如图 3 所示，主要由压控振荡器谐振单元、整形单元、分频单元、STM8 微控制器单元、温度检测单元与 D/A 转换单元组成。

作为并联谐振电路的电容器，环形探头在压控振荡器 MC1648 的作用下产生高频信号，该高频信号经过整形与分频后变成 2 ~ 4 kHz 的低频信号传送至微控制器。微控制器根据输出频率与体积含水

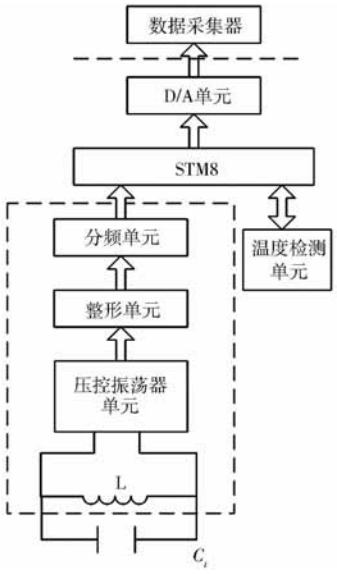

图 3　检测板系统原理框图

Fig. 3　Principle diagram of test panel system

率的归一化拟合模型，配合温度检测单元(DS18B20)获得的温度数据进行补偿后，通过数模转换模块(DAC7571)将水分检测电路的频率输出转换成 0 ~ 2 500 mV 的电压输出。

2　土壤水分传感器探头的容抗特性分析

在基于电容法的土壤水分设计过程中，环形探头的电容特性分析至关重要。本文借助一台高频网络矢量分析仪(NA7300 型，50 Ω，天津德力电子仪器公司，扫描频率 0.3 ~ 3 000 MHz、频率分辨率为 10 Hz)在 9 种介质中对环形探头的电容特性进行分析。其中测试频率选择 100 MHz，测量方法采用反射法，试验环境温度为 20℃。9 种介质及其对应介电常数如表 1 所示[23]。

表 1　有机溶液介电常数(20℃)

Tab. 1　Dielectric constant of organic solution (20℃)

介质	介电常数
空气	1.00
乙酸乙酯	6.02
异戊醇	15.19
正丁醇	17.51
异丙醇	19.92
乙醇	24.55
乙醇：水(体积比 2∶1)	43.60
乙醇：水(体积比 1∶1)	53.30
蒸馏水	81.00

首先，将试剂放入高 20 cm、直径 20 cm，中心固定有高 20 cm、直径 5.6 cm PVC 管的有机玻璃测试桶中。其次，使用 SMA 连接头将矢量网络分析的测试电缆与环形探头相连，矢量网络分析仪开机 1 h

后利用开路、短路与 50 Ω 负载校准件进行校准。最后将环形探头置于 PVC 测试管中进行电容值的测量,试验中,采用测试 5 次取平均值的方式来降低操作误差。试验结果如图 4 所示。

由图 4 曲线可以看出,环形探头电容值与周围

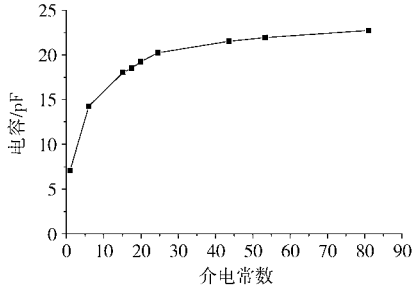

图 4 介电常数对环形探头电容特性的影响

Fig. 4 Effect of dielectric constant on capacitance characteristics of ring probe

填充介质的介电常数呈单调的非线性关系。介电常数在 0 ~ 15 区间内,曲线急剧上升,对应传感器的电容变化范围为 7.08 ~ 16.5 pF,而后曲线变化明显减缓。在介电常数为 1 ~ 81 区间内,确定传感器探头的电容值在 7.08 ~ 22.75 pF 范围内变化。

3 检测电路的测量精度试验

传感器采用并联谐振的原理检测土壤体积含水率的变化。传感器环形探头相当于电容器,谐振电感决定着土壤测试频率,考虑到传感器探头电容变化范围与测试频率受电导率等因素的影响,最终选取 102 nH 的高频绕线电感作为谐振电感。试验过程中选取 11 种高频瓷片电容模拟传感器探头接入检测电路中,测得的输出频率与电容如表 2、图 5 所示。

表 2 电容与谐振频率对应表

Tab. 2 Capacitance and resonance frequency

电容/pF	5	10	12	15	18	20	22	30	33	39	47	56
谐振频率/MHz	220.750	150.546	138.336	128.042	113.250	110.920	110.161	90.682	85.588	79.384	73.701	67.464

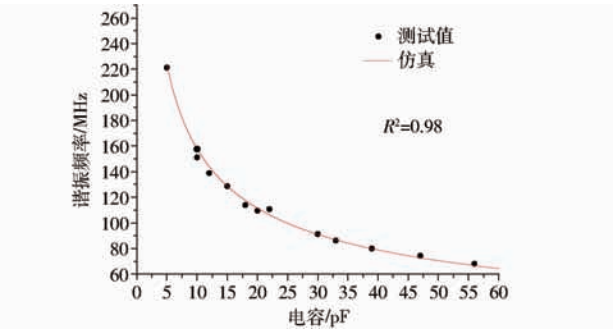

图 5 不同电容对应的谐振频率测试与运算结果

Fig. 5 Test and operation results of resonance frequency in different capacitances

由图 5 可以看出,测量电路测出结果与式(1)得出的仿真曲线决定系数达到了 0.98,说明测试电路能够准确测量感应电容大小。谐振频率随着电容的增大单调递减。传感器探头在 7.08 ~ 22.75 pF 变化范围内(土壤中的最大变化范围),谐振频率的变化范围为 188 ~ 104 MHz。根据前人的研究,在这个频率范围内可有效降低土壤盐度对测量结果的影响[24]。

4 传感器性能分析

4.1 动态响应性能试验

动态响应性能是传感器在实际应用中所关注的重要指标,表现为当传感器周围检测区域的土壤含水率发生变化时,传感器输出从变化到稳定所需要的时间。试验设备为中间固定有 PVC 管的有机玻璃筒。首先将传感器置于 PVC 管体中,测试筒中加满水,使用示波器单次触发的上升沿捕获功能,获得传感器从通电到输出稳定的时间为 50 ms。然后将传感器快速从 PVC 管体中拔出,测得传感器输出由变化到稳定的时间为 150 ms。

4.2 传感器灵敏度试验验证与标定

在传感器的设计过程中,标定是非常重要的环节。标定之前需要对水分检测电路输出的频率信号进行归一化处理。处理过程为

$$V_O = V_C \frac{f_A - f_M}{f_A - f_W} \tag{12}$$

式中 f_A——传感器在空气中时水分检测电路输出的频率

f_W——传感器在水中时输出的频率

f_M——传感器在实测土壤中输出的频率

V_C——2 500 mV 的参考电压

经过归一化处理后将传感器输出的频率信号转换成 0 ~ 2 500 mV 电压信号。

试验土样样本为取自北京林业大学苗圃(116°21′14″E、40°0′54″N)的典型粘壤土,浸出液电导率为 0.20 mS/cm,成分构成为:砂粒 11%,粉粒 71%,黏粒 18%(以上为质量分数),取回后首先自然风干过筛(孔径 0.4 mm),然后利用干燥箱(105℃,24 h)干燥。计算出配比 9 种梯度体积含水率试验样本所需水分,充分搅拌均匀,按照 1.6 g/cm^3 的土壤容重均匀装入高 20 cm、直径 30 cm,中心固定有高 40 cm、直径 5.6 cm PVC 管的 9 个 PVC 测试桶中。静置 48 h 后利用环刀取土,利用烘干法测得

9 个测试筒的体积含水率分别为 1.5%、8.05%、11.08%、18.02%、23.56%、28.77%、33.58%、36.75%与 40.01%。试验环境温度 10℃。标定环境如图 6 所示。采用专用采集设备采集传感器输出的电压，对获取到的数据进行多项式拟合，其结果如图 7 所示。

图 6　传感器的标定环境

Fig. 6　Sensor calibration environment

1. 采集器　2. 环形传感器　3. PVC 管　4. PVC 测试筒　5. RS485 转 RS232 接口　6. 便携式计算机　7. 电源

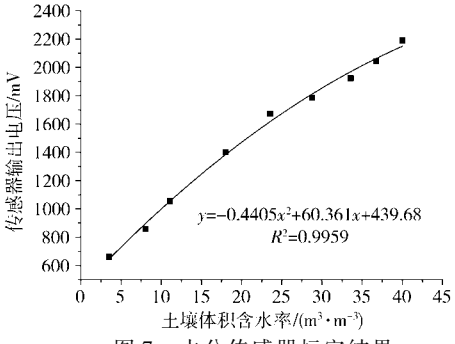

图 7　水分传感器标定结果

Fig. 7　Calibration results of moisture sensor

由图 7 可以看出，传感器的输出结果与土壤体积含水率有良好的相关性，其决定系数 R^2 达到了 0.995 9。同时可以发现传感器具有较高的灵敏性，即体积含水率每变化 10% 就有超过 600 mV 的电压输出变化。

4.3　温度对传感器输出的影响

考虑到传感器使用过程中，输出的电压受测试环境温度变化的影响，本文设计了传感器温度标定环节。

首先，将蒸馏水倒入一个直径 20 cm、高 20 cm 的 PVC 测试筒中（测试筒中心固定有高 40 cm、直径 5.6 cm 的 PVC 管）。PVC 管内放置本文所设计的土壤水分传感器，利用隔热棉将 PVC 管体的上下两端堵死以防止热量的流动。

其次，利用塑料薄膜将 PVC 测试筒密封，将水银温度计插入水中。并将 PVC 测试筒放置到干燥箱中。

最后，调节干燥箱温度在 10～50℃，以 5℃为梯度变化。使用水银温度计监测测试环境温度，当监测到的温度与干燥箱设置温度一致时，记录传感器的电压。试验结果如图 8 所示。

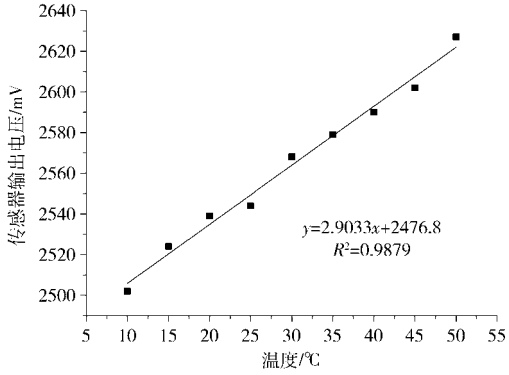

图 8　传感器输出电压受温度变化的影响

Fig. 8　Changes of sensor output with temperature

由图 8 可以看出，传感器输出电压与温度之间呈良好的线性关系，决定系数 R^2 达到了 0.987 9，温度每升高 1℃传感器大约有 2.903 3 mV 的电压升高。导致电压升高的主要原因在于探头周围填充介质的介电常数受温度影响与温度变化导致电路中电子元器件的电气特性变化。考虑到传感器输出特性受温度变化的影响，本文所设计的水分传感器配置了温度检测功能，通过实时获取环境温度对传感器输出电压进行温度补偿。为了提高传感器的通用性，水分传感器的输出接口并不提供温度的输出功能，所以本设计只针对单一水介质对传感器进行温度补偿。这种措施只能在一定程度上减小温度对传感器输出的影响，为了获取更加精确的测量数值，使用者应根据测试土壤类型建立不同梯度土壤的数学模型进行分析[22]。

4.4　传感器测量敏感性试验

4.4.1　传感器的纵向影响区域

传感器的测量敏感区域表征的是传感器在测量过程中的测量范围，是传感器性能的一个重要指标。按照 4.2 节所示方法配置体积含水率为 16%、20%与 25% 3 种梯度的试验土壤。将配置好的试验土壤依次装入高 20 cm、直径 30 cm 的 3 个测试桶中（中心固定有高 40 cm、直径 5.6 cm 的 PVC 测试管）。使用保鲜膜密封静置 64 h 备用。

将本文所设计的土壤水分传感器置于配置好的土体 PVC 管体中，传感器的中心距离土体上表面 10 cm，以 1 cm 为梯度将传感器向上移动，并记录每个梯度传感器的电压。3 种不同含水率土体的试验结果如图 9 所示。

由图 9 可以看出，传感器在 PVC 管体内上移的过程中，传感器输出的电压随着距离的增加单调减小，测试土壤的体积含水率对传感器的纵向影响区

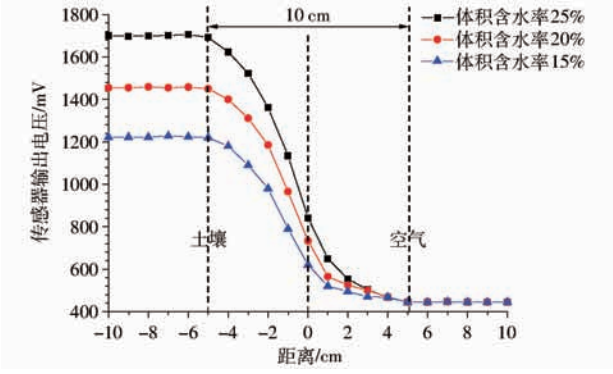

图 9 传感器纵向影响范围的试验结果

Fig. 9 Experimental results of axial sensitivity for sensors

域并没有太大的影响,其纵向测试范围为 10 cm,为了确保测量数据的准确性,本文所设计的传感器应置于距离土壤表面 5 cm 以下处进行测量。

4.4.2 传感器的横向影响区域

将本文所设计土壤水分传感器至于 PVC 测试管中,以 1 cm 为梯度利用土刀环周削薄测试筒中土壤的厚度(PVC 测试管的管壁至土壤边缘的距离),并记录传感器输出的电压。试验过程如图 10 所示。

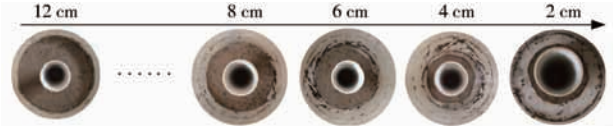

图 10 传感器影响半径测量的试验过程

Fig. 10 Experiment of relative radial sensitivity measurement of sensors

为了更加直观地表现土体厚度对传感器输出电压的影响,提出能量指数 K_a 来表征传感器的横向半径中能量的分布状况。

$$K_a = \frac{V_C - V_{PVC}}{V_{soil} - V_{PVC}} \tag{13}$$

式中 V_{soil}——传感器在 12 cm 厚度土壤中的电压

V_{PVC}——传感器在 PVC 管体中的电压(PVC 管体周围为空气)

V_C——传感器测量的实时值

传感器在体积含水率为 16%、20% 与 25% 3 种梯度的试验土壤中测得的试验结果如图 11 所示。

由图 11 可以看出,能量指数 K_a 随着周围土壤厚度的增加而变大。对于 3 种梯度的试验土壤,99% 的能量均匀分布在距离 PVC 测试管外壁 5 cm 左右的土壤范围内。因此本文所设计的非接触式土壤水分传感器的横向影响范围为 5 cm。

5 对比试验与结果分析

为了分析土壤非接触式传感器与国外此类产品性能差距,设计了传感器对比试验。对比的传感器为澳大利亚 Sentek 公司的 EnviroSCAN 型土壤水分扩线系统,其测量范围为 0 ~ 100%,精度为 ±2%。

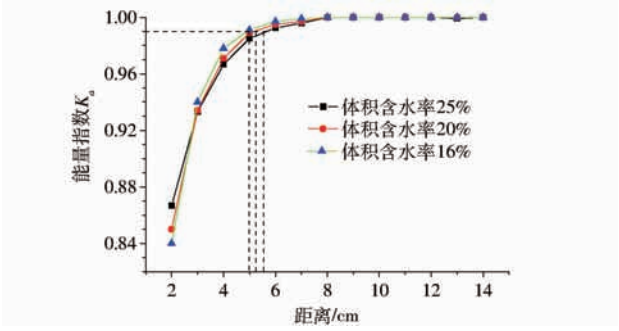

图 11 传感器影响半径测量的试验结果

Fig. 11 Experimental results of relative radial sensitivity of sensors

按照 4.2 节的试验步骤配置体积含水率为 5.4%、10.4%、16.3%、23.9%、28.6%、32.3%、36.5% 7 种土样,利用 2 种传感器进行分别测量。土壤非接触式传感器与 EnviroSCAN 土壤水分扩线系统测得的数据结果如表 3 所示。

表 3 与 EnviroSCAN 土壤水分扩线系统的对比

Tab. 3 Comparative experiments with EnviroSCAN soil moisture systems %

编号	1	2	3	4	5	6	7
EnviroSCAN	5.32	10.61	17.11	24.51	27.65	33.56	36.22
自制传感器	5.43	9.92	16.01	23.31	28.62	32.28	35.57
绝对误差	-0.11	0.69	1.10	1.20	-0.63	1.28	0.65
相对误差	-2.1	6.5	6.4	4.9	-2.3	3.8	1.8

从表 3 可以看出,体积含水率的绝对误差为 -0.63% ~ 1.20%,相对误差为 -2.3% ~ 6.5%。两者间的绝对误差小于 2%,表明 2 个传感器的性能相当。

6 结论

(1)设计了一种土壤水分非接触式传感器,可实现对土壤水分的实时监测。

(2)对传感器环形探头的电容特性与检测电路的性能进行了研究,借助网络矢量分析仪,在 9 种有机溶液中对环形探头的电容特性进行了分析,确定了环形探头在介电常数从 1 ~ 81 的区间内,探头表征电容变化范围为 7.08 ~ 22.75 pF。通过与 11 种容值高频瓷片电容的并联谐振试验,证明传感器的检测电路精度能够满足传感器设计的要求。

(3)从试验标定与相关试验结果可以看出,传感器的精度、灵敏度与动态响应性能均能满足传感器的设计要求。

(4)提出了能量指数 K_a,通过试验的方法得出传感器测量范围,纵向影响范围为 10 cm,横向影响范围为 5 cm。

(5)传感器的对比试验表明,本文所设计的非接触式土壤水分传感器的检测精度与国外同类产品相当。体积含水率的绝对误差为 -0.63% ~1.20%,相对误差为 -2.3% ~6.5%。

参 考 文 献

1 李连骏,孙宇瑞,林剑辉. 一种太阳能供电的土壤水分无线传感器[J]. 江苏大学学报:自然科学版,2009,30(6):541 -544.
LI Lianjun, SUN Yurui, LIN Jianhui. A wireless-sensor for soil water content powered by solar energy[J]. Journal of Jiangsu University: Natural Science Edition, 2009, 30(6): 541 -544. (in Chinese)

2 KANG S, ZHANG J. Controlled alternate partial root-zone irrigation: Its physiological consequences and impact on water use efficiency[J]. Journal of Experimental Botany, 2004, 55(407): 2437 -2446.

3 HUTTON R J, LOVEYS B R. A partial root zone drying irrigation strategy for citrus-effects on water useefficiency and fruit characteristics[J]. Agricultural Water Management, 2011, 98(10):1485 -1496.

4 HEDLEY C B, YULE I J. A method for spatial prediction of daily soil water status for precise irrigation scheduling[J]. Agricultural Water Management, 2009, 96(12): 1737 -1745.

5 THOMPSON R B, GALLARDE M, VALDEZ L C, et al. Using plant water status to define threshold values for irrigation management of vegetable crops using soil moisture sensors[J]. Agricultural Water Management, 2007, 88(1 -3):147 -158.

6 GAO Xiaodong, WU Pute, ZHAO Xining, et al. Estimating the spatial means and variability of root-zone soil moisture in gullies using measurements from nearby uplands[J]. Journal of Hydrology, 2013, 476(1): 28 -41.

7 张学礼,胡振琪,初士立. 土壤含水量测定方法研究进展[J]. 土壤通报,2005,36(1):118 -121.
ZHANG Xueli, HU Zhenqi, CHU Shili. Methods for measuring soil water content: a review[J]. Chinese Journal of Soil Science, 2005, 36(1): 118 -121. (in Chinese)

8 蔡坤,岳学军,洪添胜,等. 基于 RC 网络相频特性的土壤含水率传感器设计[J]. 农业工程学报,2013,29(7):36 -43.
CAI Kun, YUE Xuejun, HONG Tiansheng, et al. Design of soil water content sensor based on phase-frequency characteristics of RC networks[J]. Transactions of the CSAE, 2013, 29(7): 36 -43. (in Chinese)

9 DEAN T J, BELL J P, BATY A J B. Soil moisture measurement byan improved capacitance technique: Part I. sensor design and performance[J]. Journal of Hydrology,1987, 93(1 -2): 67 -78.

10 PALTINEANU I C, STARR J L. Real-time soil water dynamics using multi sensor capacitance probes: Laboratory calibration[J]. Soil Science Society of America Journal,1997,61(6):1576 -1585.

11 SHENG W, SUN Y, LAMMERS P S, et al. Observing soil water dynamics under two field conditions by a novel sensor system [J]. Journal of Hydrology,2011,409(1 -2):555 -560.

12 李晓东,吴永烽,李光林,等. 基于太阳能的无线土壤水分传感器的研制[J]. 农业工程学报,2010,26(11):13 -18.
LI Xiaodong, WU Yongfeng, LI Guanglin, et al. Development of wireless soil moisture sensor based on solar energy[J]. Transactions of the CSAE, 2010,26(11):13 -18. (in Chinese)

13 赵燕东,马扬飞,王勇志. 绿地精准灌溉控制系统设计与最优灌溉量分析[J]. 农业机械学报,2012,43(3):46 -50.
ZHAO Yandong, MA Yangfei, WANG Yongzhi. Green land precision irrigation control system and analysis of optimal irrigation amount[J]. Translations of the Chinese Society for Agricultural Machinery, 2012, 43(3):46 -50. (in Chinese)

14 STEVEN R, ROBERT C, JOAQUIN J, et al. Soil water sensing for water balance, ET and WUE[J]. Agricultural Water Management,2012,104(2):1 -9.

15 赵燕东,王一鸣. 智能化土壤水分分布速测系统[J]. 农业机械学报,2005,36(2):76 -78.
ZHAO Yandong, WANG Yiming. Intelligent system of measuring the spatial distributions of Soil moisture[J]. Transactions of the Chinese Society for Agricultural Machinery, 2005,36(2):76 -78. (in Chinese)

16 彭曾愉,赵燕东. 基于 μC/OS -Ⅱ操作系统的土壤水分实时监测系统[J]. 北京林业大学学报,2010,32(6):114 -119.
PENG Zengyu, ZHAO Yandong. A monitoring system of real-time soil water content based onμC/OS -Ⅱ operating system[J]. Journal of Beijing Forestry University, 2010,32(6):114 -119. (in Chinese)

17 GASKIN G J, MILLER J D. Measurement of soil water content using a simplified impedance measuring technique[J]. Journal of Agricultural Engineering Research, 1996, 63(2): 153 -159.

18 VELAZQUEZ M B, GRACIA L C, PLAZA G P J. Determination of dielectric properties of agricultural soil[J]. Biosystems Engineering, 2005,91(1): 119 -125.

19 KIZITI F, CAMPBELL C S, CAMPBELL G S, et al. Frequency, electrical conductivity and temperature analysis of a low-cost capacitance soil moisture sensor[J]. Journal of Hydrology, 2008,352(3 -4): 367 -378.

20 WOJCIECH S, ANDRZEJ W. A FDR sensor for measuring complex soil dielectric permittivity in the 10 ~500 MHz frequency range[J]. Sensors, 2010,10(4): 3314 -3329.

21 MA Daokun, SUN Yurui, WANG Maohua, et al. Three-dimensional numerical modeling of a four-pin probe for soil water content [J]. Australian Journal of Soil Research, 2006,44(2):183 -189.

22 高志涛,刘卫平,赵燕东,等. 多层土壤剖面复合传感器设计与性能分析[J]. 农业机械学报,2016,47(1):108 -117.
GAO Zhitao, LIU Weiping, ZHAO Yandong, et al. Design and performance analysis of a multilayer composite sensor for soil profile [J]. Transactions of the Chinese Society for Agricultural Machinery, 2016,47(1):108 -117. (in Chinese)

23 赵燕东, 高超,张新,等. 基于驻波率原理的植物茎体水分无损检测方法研究[J]. 农业机械学报,2016,47(1):310 -316.
ZHAO Yandong, GAO Chao, ZHANG Xin, et al. Non-destructive measurement of plant stem water content based on standing wave ratio [J]. Transactions of the Chinese Society for Agricultural Machinery, 2016,47(1):310 -316. (in Chinese)

24 NADLER A, LAPID Y. An improved capacitance sensor for in situ monitoring of soil moisture[J]. Soil Research,1996,34(3): 361 -368.